Dalton Transactions

Accepted Manuscript

This article can be cited before page numbers have been issued, to do this please use: H. Tian, H. Shimakoshi, S. Kim, G. Park, Y. You and Y. Hisaeda, *Dalton Trans.*, 2017, DOI: 10.1039/C7DT03742B.

This is an Accepted Manuscript, which has been through the Royal Society of Chemistry peer review process and has been accepted for publication.

Accepted Manuscripts are published online shortly after acceptance, before technical editing, formatting and proof reading. Using this free service, authors can make their results available to the community, in citable form, before we publish the edited article. We will replace this Accepted Manuscript with the edited and formatted Advance Article as soon as it is available.

You can find more information about Accepted Manuscripts in the author guidelines.

Please note that technical editing may introduce minor changes to the text and/or graphics, which may alter content. The journal's standard Terms & Conditions and the ethical guidelines, outlined in our author and reviewer resource centre, still apply. In no event shall the Royal Society of Chemistry be held responsible for any errors or omissions in this Accepted Manuscript or any consequences arising from the use of any information it contains.

ROYAL SOCIETY OF CHEMISTRY

rsc.li/dalton

View Article Online
DOI: 10.1039/C7DT03742B

Journal Name

ARTICLE

Photocatalytic Function of B_{12} Complex with Cyclometalated Iridium(III) Complex as Photosensitizer under Visible Light Irradiation†

Received 00th January 20xx,
Accepted 00th January 20xx

DOI: 10.1039/x0xx00000x

www.rsc.org/

Hui Tian,[a] Hisashi Shimakoshi,*[a] Sinheui Kim,[b] Gyurim Park,[b] Youngmin You*[b] and Yoshio Hisaeda*[a]

A visible light induced three-component catalytic system with the cobalamin derivative (B_{12}) as a catalyst, the cyclometalated iridium(III) complex (Irdfppy, Irppy, Irpbt and $[Ir\{dF(CF_3)ppy\}_2(dtbpy)]PF_6$ as a photosensitizer and triethanolamine as an electron source under N_2 was developed. This catalytic system showed a much higher catalytic efficiency than the previous catalytic system using $[Ru(bpy)_3]Cl_2$ as the photosensitizer for the dechlorination reaction of 1,1-bis(4-chlorophenyl)-2,2,2-trichloroethane (DDT). Noteworthy is the fact that the remarkable high turnover number (over ten thousand) based on B_{12}, which ranks at the top among the reported studies, was obtained when Irdfppy was used as a photosensitizer. This photocatalytic system was also successfully applied to the B_{12} enzyme-mimic reaction, i.e., the 1,2-migration of the phenyl group of 2-bromomethyl-2-phenylmalonate. The plausible reaction mechanism was proposed, which involved two quenching pathways, an oxidative quenching pathway and a reductive quenching pathway, to be responsible for the initial electron transfer of the excited-state photosensitizers during the DDT dechlorination reaction. Transient photoluminescence experiments revealed that oxidative quenching of the photosensitizer dominated over the reductive quenching pathway.

Introduction

The cobalamin derivative (B_{12}) has emerged in a variety of enzymes, such as methylmalonl CoA mutase, methionine synthase, ribonucleotide reductase, epoxyqueosine reductase and reductive dehalogenase as a cofactor.[1] Inspired by the unique dehalogenation function of B_{12} in the reductive dehalogenase, B_{12} model complexes have been widely studied as excellent catalysts for the dehalogenation reactions since the Co(I) species of the B_{12} complexes are supernucleophlic and can react with alkyl halides to generate alkylated complexes which provide the dehalogenation products.[2]

Organic halides are indispensable chemicals that are widely utilized as general organic solvents, useful reagents for organic synthesis etc., both in laboratory studies and industrial production.[3] It is noted that their wastes have caused environmental contamination and several health problems due to their accumulation in the environment and biomagnificaition properties in living organisms.[4] To solve these problems, the reductive dehalogenation of organic halides has been intensively studied for decades[5]. In recent years, our group reported smart dechlorination systems of 1,1-bis(4-chlorophenyl)-2,2,2-trichloroethane (DDT) catalyzed by the B_{12} complex in the presence of a photosensitizer ($[Ru(II)(bpy)_3]Cl_2$) or its derivatives under visible light irradiation.[6] In this system, the supernucleophlic Co(I) species was generated from the reduction of the Co(II) state of the B_{12} derivative by electron transfer from the photosensitizer by visible light irradiation. Although this reaction system worked well, low turnovers based on the B_{12} complex were obtained even though an excess amount of the photosensitizer was used. It is noted that Yoon and co-workers reported the decomposition pathway and fate of $Ru(bpy)_3^{2+}$ during the photocatalytic reaction, in which rapid decomposition of the $Ru(bpy)_3^{2+}$ complex under light irradiation was demonstrated.[7] Furthermore, Sun's work revealed that the excited state of $Ru(bpy)_3^{2+}$ in the photocatalytic system cannot be effectively reduced even with a large excess of reductant.[8] The fast decomposition and inefficient reductive quenching of $Ru(bpy)_3^{2+}$ during the catalytic reaction may be the factors that led to limited turnovers of B_{12} combined the use with the Ru photosensitizer. Therefore, there are still efforts that should be made to develop more efficient and robust visible light responsible photosensitizers to improve the catalytic efficiency of the B_{12} complex in the photocatalytic system.

Cyclometalated iridium(III) complexes have been rapidly developing due to their superior photophysical and photochemical properties.[9] Consequently, they have been widely utilized as photoredox catalysts in organic synthesis as

[a] Department of Chemistry and Biochemistry, Graduate School of Engineering, Kyushu University, Motooka, Fukuoka 819-0395, Japan. E-mail: shimakoshi@mail.cstm.kyushu-u.ac.jp, yhisatcm@mail.cstm.kyushu-u.ac.jp; Fax: +81-92-802-2828; Tel: +81-92-802-2828
[b] Division of Chemical Engineering and Materials Science, Ewha Womans University, Seoul 03760, Republic of Korea. E-mail: odds2@ewha.ac.kr

†Electronic Supplementary Information (ESI) available: [Figure S1-S8]. See DOI: 10.1039/x0xx00000x

View Article Online
DOI: 10.1039/C7DT03742B

well as serving as photosensitizers. [10] It has been recognized that $[Ir(C^N)_2(N^N)]^+$ chromophores (C^

N=cyclometallating ligand and N^N=bidendate N2 ligand) display considerably higher efficiencies with remarkable high turnovers in homogeneous H_2-evolving photocatalytic systems working as photosensitizer than that obtained from the typical metal bipyridyl complexes such as the $Ru(bpy)_3^{2+}$ complex.[8,11] Bernhard's group systematically studied the catalytic efficiency improvement by evaluating the photophysical parameters and pointed out the longer excited-state lifetimes and improved stability of the $[Ir(C^N)_2(N^N)]^+$ complexes that contributed to their high efficiency.[12]

In this study, a three-component catalytic system involving the B_{12} complex as a catalyst, cyclometalated iridium(III) complexes as a photosensitizer, and triethanolamine (TEOA) as a sacrificial reductant is reported. This catalytic system was applied to the visible light-driven dehalogenation of DDT, which is one of the most problematic POPs (persistent organic pollutants).[13] A high catalytic efficiency with significantly enhanced turnovers was obtained. The 1,2-migration of the phenyl group of 2-bromomethyl-2-phenylmalonate was also conducted as a model reaction of the B_{12} dependent enzyme.

Experimental

Materials

All solvents and chemicals used in this study were of reagent grade. Unless otherwise noted, commercial reagents, including $[Ir\{dF(CF_3)ppy\}_2(dtbpy)]PF_6$ ([iridium bis(2-(2,4-difluorophenyl)-5-trifluoromethylpyridinate) (2,2′-(4,4′-di(*t*-butyl)bipyridine))]hexafluorophosphate) and $[Ru(II)(bpy)_3]Cl_2$ (bpy = 2,2'-bipyridine), were purchased from WAKO, Aldrich, and other commercial suppliers and were used as received. Heptamethyl cobyrinate perchlorate, the B_{12} complex, was synthesized by a previously reported method.[14,15] The cobalt complex, $Co(III)(DO)(DOH)Br_2$, was prepared according to the literature.[16] Bicyclometalated iridium(III) complexes, Irdfppy ([iridium bis(2-(2,4-difluorophenyl)pyridinate) (9,10-phnanthroline)]hexafluorophosphate), Irppy ([iridium bis(2-phenylpyridinate) (9,10-phnanthroline)]hexafluorophosphate), and Irpbt ([iridium bis(2-phenylbenzo[*d*]thiazolate) (9,10-phnanthroline)]hexafluorophosphate), were prepared following previously described methods[17] (Scheme 1). 2-Bromomethyl-2-phenylmalonate (**1**) and the authentic sample, diethyl 2-methyl-2-phenylmalonate (**3**), were synthesized according to our previous report.[18] Diethylbenzylmalonate (**2**) was purchased from TCI.

Measurements

The NMR spectra were recorded by a Bruker Avance 500 spectrometer at the Center of Advanced Instrumental Analysis of Kyushu University, and the chemical shifts (in ppm) were referenced relative to the residual protic peaks of the solvents. The GC-mass spectra (GC-MS) were obtained using a Shimadzu GC-QP5050A equipped with a J&W Scientific DB-1 column (length 30 m; ID 0.25 mm, film 0.25 μm). The UV-vis absorption spectra were measured by a Hitachi U-3300 spectrophotometer at room temperature. The MALDI-TOF mass spectra were obtained by a Bruker autoflex II using dithranol as the matrix. The cyclic voltammograms (CV) were obtained using a BAS CV 50W electrochemical analyzer. A three-electrode cell equipped with 1-mm diameter platinum wires as the working and counter electrodes were used. An Ag/AgCl (3.0 M NaCl aq.) electrode served as the reference in the presence of tetrabutylammonium perchlorate (n-Bu_4NClO_4) as the supporting electrolyte. The $E_{1/2}$ value of the ferrocene–ferrocenium (Fc/Fc^+) was 0.41 V *vs*. Ag/AgCl with this setup. Fluorescence emission spectra were collected at room temperature by a Hitachi F-7000 fluorescence spectrometer at the scan speed of 240 nm/min, and the slits were set at 5.0 nm unless otherwise noted. The excitation wavelength was 264 nm. An ASAHI SPECTRA MAX-301 with band-pass filters was used as monochromatic light source. The power of the light source was measured by an Optical Power Meter, Model 1916-R (Newport).

Photophysical studies of photosensitizers with B_{12} complex

A 100 μM photosensitizer in Ar-saturated CH_3CN was used for the determination of the rate constant for quenching (k_q) of a photosensitizer. Photoluminescence decay traces of the photosensitizers were acquired based on time-correlated single-photon-counting (TCSPC) techniques using a FluoTime 200 instrument (PicoQuant, Germany) after a picosecond pulsed laser excitation. A 377 nm diode laser (PicoQuant, Germany) was used as the excitation source. The photoluminescence signals at the emission peak wavelengths of the photosensitizers were obtained through an automated motorized monochromator. Photoluminescence decay profiles were analyzed (OriginPro 8.0, OriginLab) using single or double exponential decay models. In the case of the biphasic decays, the photoluminescence lifetime (τ_{obs}) values were calculated from the relationship $\tau_{obs} = \Sigma A_i\tau_i^2/\Sigma A_i\tau_i$ (i = 1–2), where A_i and τ_i are the pre-exponential factor and the time constant, respectively. The τ_{obs} values were determined with the increasing concentration of the B_{12} complex or TEOA under a pseudo first order condition. The quenching rates were calculated from the relationship, quenching rate = $1/\tau_{obs} - 1/\tau_{obs}(0)$, where τ_{obs} and $\tau_{obs}(0)$ correspond to the photoluminescence lifetimes of a photosensitizer in the presence and absence of the B_{12} complex or TEOA, respectively. A linear fit of the quenching rate *vs* the concentration of the B_{12} complex or TEOA yielded the k_q value.

General procedure of catalytic reaction

A 10 mL ethanol solution of the B_{12} complex (1.0×10^{-5} M), iridium(III) complex (0.128×10^{-5} M), TEOA (0.25 M) and DDT (3.0×10^{-3} M) was degassed by N_2 gas, then the solution was stirred at room temperature under irradiation using a 200 W tungsten lump with a 420 nm cut-off filter (Sigma Koki, 42 L) and a heat cut-off filter (Sigma Koki, 30 H). After the reaction, the solution was first evaporated to remove the solvent, then water (40 ml) and $CHCl_3$ (30 ml) were added to the residue for extraction. The chloroform layer was washed 3 times with water and dried with anhydrous Na_2SO_4. After filtration and vacuum drying, the residue was passed through a silica gel short column eluting with $CHCl_3$ to remove the B_{12} and iridium(III) complexes. The product for the DDT dechlorination reactions was analyzed by employing GC-MS or ^1H NMR with 1,4-dioxane as the internal standard.

View Article Online
DOI: 10.1039/C7DT03742B

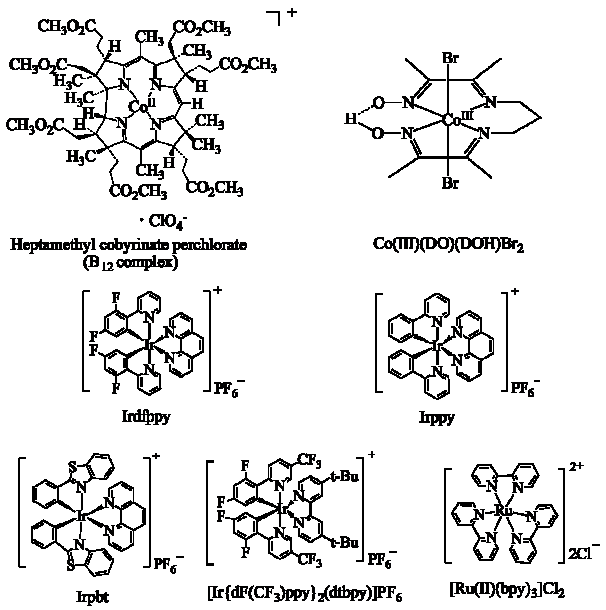

Scheme 1 Structure of B_{12} complex, Co(III)(DO)(DOH)Br$_2$, Irdfppy, Irppy, Irpbt, [Ir{dF(CF$_3$)ppy}$_2$(dtbpy)]PF$_6$ and [Ru(II)(bpy)$_3$]Cl$_2$.

Results and discussion

In this study, heptamethyl cobyrinate perchlorate (B_{12} complex) and another model compound of B_{12}, Co(III)(DO)(DOH)Br$_2$, were employed as catalysts for the dechlorination reaction. Four iridium(III) complexes (i.e., Irdfppy, Irppy, Irpbt and [Ir{dF(CF$_3$)ppy}$_2$(dtbpy)]PF$_6$) and the conventional [Ru(II)(bpy)$_3$]Cl$_2$ were used as photosensitizers.

The UV-vis absorption spectra of the B_{12} complex, Co(III)(DO)(DOH)Br$_2$, the cyclometalated iridium(III) complexes (i.e., Irdfppy, Irppy, Irpbt and [Ir{dF(CF$_3$)ppy}$_2$(dtbpy)]PF$_6$) and [Ru(II)(bpy)$_3$]Cl$_2$ in ethanol are shown in Fig. 1. The B_{12} complex showed the typical absorption band of the Co(II) species of the cobalamin derivative around 480 nm (Fig. 1a) and all photosensitizers exhibited broad absorptions in the visible region.[19]

The ground-state redox potentials of the B_{12} complex, Irdfppy, Irppy, Irpbt, [Ir{dF(CF$_3$)ppy}$_2$(dtbpy)]PF$_6$ and [Ru(II)(bpy)$_3$]Cl$_2$ as well as the oxidation potential of a sacrificial reductant, TEOA, were

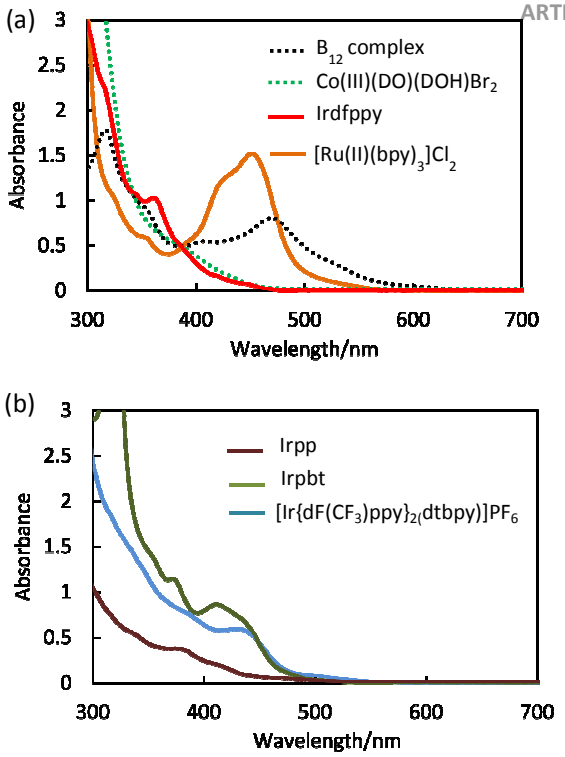

Fig. 1 UV-vis absorption spectra of B_{12} complex, Co(III)(DO)(DOH)Br$_2$, [Ru(II)(bpy)$_3$]Cl$_2$ and Irdfppy (a), Irppy, Irpbt and [Ir{dF(CF$_3$)ppy}$_2$(dtbpy)]PF$_6$ (b) in ethanol (1.28×10^{-4}M).

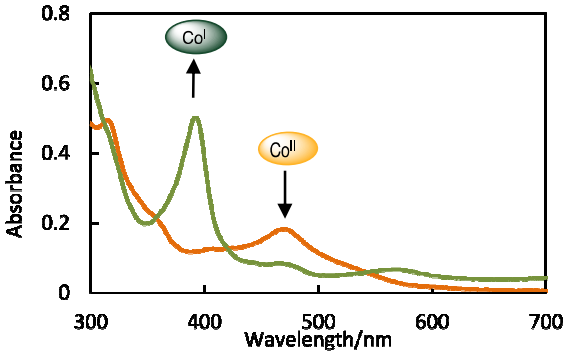

Fig. 2 UV-vis spectral change of B_{12} complex (2.5×10^{-5} M) in ethanol in the presence of Irdfppy (0.32×10^{-5} M) and TEOA (0.5 M) by visible light irradiation (λ≥420 nm): before irradiation (yellow line) and after irradiation for 2 hours (green line).

Table 1 Excited-state and ground state redox potentials of B_{12} complex, Irdfppy, Irppy, Irpbt, [Ir{dF(CF$_3$)ppy}$_2$(dtbpy)]PF$_6$, [Ru(II)(bpy)$_3$]Cl$_2$ and TEOA

Potenial/V	B_{12} complex	Irdfppy	Irppy	Irpbt	[Ir{dF(CF$_3$)ppy}$_2$(dtbpy)]PF$_6$	[Ru(II)(bpy)$_3$]Cl$_2$	TEOA
E_{ox}*[a]	-	-1.17	-0.90	-1.12	-1.02	-0.73[b]	-
E_{red}*[a]	-	1.47	0.90	1.21	1.52	0.73[b]	-
E_{ox}[c]	0.53($Co^{III/II}$)	1.63	1.32	1.49	1.78	0.95	0.93
E_{red}[c]	-0.61($Co^{II/I}$)	-1.22	-1.28	-1.24	-1.28	-1.30	-

[a]Reference (20). [b]reference (11a). [c]Condition: [complex] = 1.0×10^{-3}M, [n-Bu$_4$NClO$_4$]= 1.0×10^{-1}M, [solvent]= acetonitrile, using a Pt wire as counter electrode, Pt with 1 mm diameter as working electrode, Ag/AgCl (3.0 M NaCl aqueous) as reference electrode at room temperature, potential V *vs.* Ag/AgCl; ground state potentials were determined by CV measurement in CH$_3$CN.

View Article Online
DOI: 10.1039/C7DT03742B

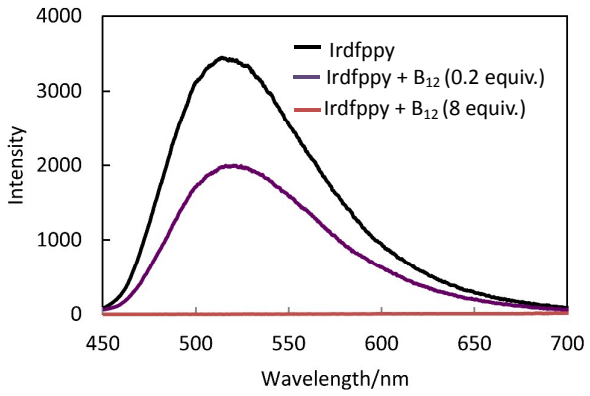

Fig. 3 Emission spectra of Irdfppy (black line), and spectra change with adding different amount of B_{12} complex: 0.2 equiv. mole (purple line), 8 equiv. mole (brown line) at room temperature with a 37L filter in ethanol; λ_{ex}=264 nm, [Irdfppy]= 0.128×10^{-5} M.

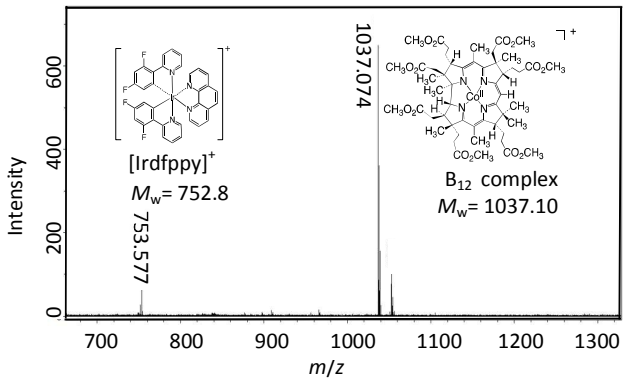

Fig. 4 MALDI-TOF mass spectrum of B_{12} complex and Irdfppy after catalytic reaction.

determined by cyclic voltammetry in acetonitrile solutions (Fig. S1). The results along with the excited-state redox potentials (E_{ox}^* and E_{red}^*) of Irdfppy, Irppy, Irpbt and $[Ir\{dF(CF_3)ppy\}_2(dtbpy)]PF_6$ are summarized in Table 1. The electrochemical potentials reveal that all the photosensitizers are capable of reduction of the B_{12} complex into a supernucleophilic Co(I) species by electron transfer from the excited state (oxidative quenching) and the one-electron-reduced state (reductive quenching).

The reductive formation of the Co(I) species of the B_{12} complex was monitored by UV-vis spectroscopy in the presence of Irdfppy and TEOA under visible light irradiation (λ≥420 nm). After visible light irradiation for 2 hours, the peak of the Co(II) species (yellow line) disappeared and a strong absorption at 390 nm was observed (green line) as shown in Fig. 2, which is the typical peak of the Co(I) species of the B_{12} complex.[5b] This result suggested that the B_{12} complex was reduced to the Co(I) species by photoinduced electron transfer from Irdfppy. This notion is supported by the phosphorescence quenching experiments shown in Fig. 3 .

The phosphorescence intensity of Irdfppy in proportion to the added concentration of B_{12} complex is displayed in Fig.3. Complete quenching was observed in the presence of 8 equiv. of the B_{12} complex. The absence of any spectral shift in the phosphorescence spectra suggested diffusional quenching of Irdfppy by the B_{12} complex. Taken together, these spectroscopic behaviors indicated the occurrence of oxidative quenching of Irdfppy by the B_{12} complex. Electron transfer processes between the two complexes will be discussed later (*vide infra*).

The catalytic performance of this photoreaction system was evaluated using DDT as a substrate. The results are summarized in Table 2. When DDT was irradiated with visible light in the presence of the B_{12} complex, Irdfppy and TEOA, the dichlorination reaction of DDT efficiently proceeded as shown in Entry 1 of Table 2. DDT

Table 2 Photocatalytic dechlorination of DDT by B_{12} complex with Irdfppy as photosensitizer[a]

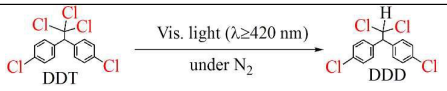

Entry	Conversion (%)	Yiled (%)	TON1	TON2
1	100	93	279	2180
2[b]	0	0	-	-
3[c]	18	14	42	-
4[d]	0	0	-	-
5[e]	0	0	-	-
6[f]	43	29	87	680
7[g]	93	90	10880	84375

[a]Condition: $[B_{12}$ complex$]=1.0\times10^{-5}$ M, [Irdfppy]$=0.128\times10^{-5}$ M (0.128 equiv. mole), [TEOA]=0.25 M, [DDT]$=3.0\times10^{-3}$ M (300 equiv. mole), solvent: ethanol, reaction time: 3 hours, light source: 200 W tungsten lump with L42 cut-off filter ($\lambda \geq 420$ nm) at 5 cm distance. Conversion and yield were based on the initial concentration of the substrate. Turnover number 1 (TON1) is based on the B_{12} complex, TON2 is based on Irdfppy. [b]No B_{12} complex. [c]No Irdfppy. [d]No TEOA. [e]In the dark. [f]$Co(DO)(DOH)Br_2$ was used in place of the B_{12} complex. [g][TEOA]=2.5 M, [DDT]=0.12 M, reaction time was 36 hours.

Table 3 Dechlorination of DDT with different photosensitizers[a]

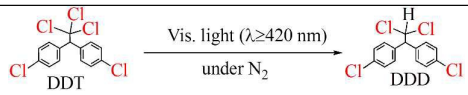

Entry	Photosensitizer	Conversion(%)	Yield (%)	TON1	TON2
1	Irdfppy	100	93	279	2180
2[b]	Irppy	90	67	201	1570
3[c]	Irpbt	100	84	252	1968
4[d]	$[Ir\{dF(CF_3)ppy\}_2(dtbpy)]PF_6$	100	91	273	2132
5	$[Ru(II)(bpy)_3]Cl_2$	28	26	78	609

[a]Condition: $[B_{12}$ complex$]=1.0\times10^{-5}$ M, [photosensitizer]$=0.128\times10^{-5}$ M (0.128 equiv. mole), [TEOA]=0.25 M, [DDT]$=3.0\times10^{-3}$ M (300 equiv. mole), solvent: ethanol, reaction time: 3 hours, light source: 200 W tungsten lump with L42 cut-off filter ($\lambda \geq 420$ nm) at 5cm distance. Conversion and yield were based on the initial concentration of the substrate and calculated by ^{1}H NMR. Turnover number 1 (TON1) is based on [B_{12} complex], TON2 is based on [photosensitizer]. [b]DDA (9%), TTBD(*E*) (7%), [c]DDA (4%), TTBD(*E*) (4%), DDMU (1%), [d]DDA (3%), TTDB(*E*)(1%)..

View Article Online
DOI: 10.1039/C7DT03742B

was almost completely dichlorinated to the monodechlorinated product, 1,1-bis(4-chlorophenyl)-2,2-dichloroethane (DDD), after 3 hours of visible light irradiation.[‡] The turnover numbers (TONs) based on the B_{12} complex and Irdfppy reached 279 and 2180, respectively. In contrast, the reaction almost did not proceed under the conditions without B_{12}, Irdfppy, TEOA, or visible light irradiation (Entries 2, 3, 4 and 5, respectively, in Table 2).[§] When Co(III)(DO)(DOH)Br_2 was conducted as a catalyst in place of the B_{12} complex, the yield of DDD was only 29% (Entry 7 in Table 2) due to the poor stability of the Co(III)(DO)(DOH)Br_2.[§§]

The stability of the B_{12} complex was confirmed by the detection of the UV-vis spectral change before and after the catalytic reaction (Fig. S2). The intensity of the Co(II) species peak of B_{12} complex showed a slight change, which indicated that most of the B_{12} complex survived from the catalytic reaction. The MALDI-TOF mass spectrometric analysis was also conducted after the catalytic reaction. Mass peaks ascribed to the B_{12} complex together with Irdfppy were clearly detected as shown in Fig. 4. Thus, the B_{12} complex and Irdfppy are very stable compounds during the photocatalytic reactions. These results further suggested that higher TONs might be achieved under the present reaction conditions due to the high stability of both compounds. To confirm this, the reaction was conducted for 36 hours with increasing concentrations of DDT to 0.12 M and TEOA to 2.5 M. Noteworthy, the TONs were significantly increased to 10,880 and 84,375 based on the B_{12} complex and Irdfppy, respectively, among the highest reported TONs (Entry 7, Table2).

To confirm that the catalysis was due to photon absorption by Irdfppy, we determined the action spectrum of the catalytic dechlorination of DDT. A Xenon light source with band-path filters was utilized to provide monochromatic lights at 350 nm, 365 nm, 400 nm, 490 nm, 540 nm and 600 nm with the same light intensity of 1.9 mW/cm^2. The action spectrum, which plots the yields determined at the irradiation wavelengths, was depicted together with the UV-vis absorption spectra of the B_{12} complex (red line) and Irdfppy (black line) in Fig. 5. The similarity between the action spectrum and the spectral profiles of Irdfppy suggested that the desired photosensitizing reaction by Irdfppy actually occurred to allow the catalytic reaction.

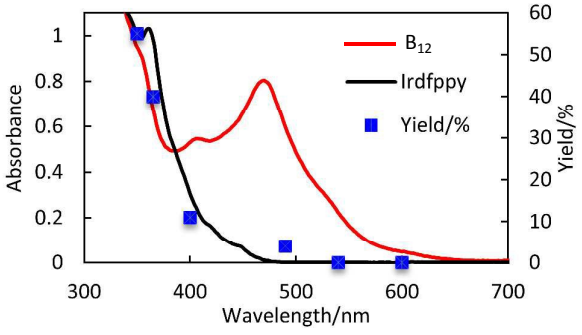

Fig. 5 Action spectrum of B_{12}-Irdfppy catalytic system: UV-vis spectra of B_{12} complex (red line) and Irdfppy (black line), yield of DDD at corresponding wavelength (blue square).

Table 4 Catalytic reaction of 2-bromomethyl-2-phenylmalonate by B_{12} complex with Irdfppy as photosensitizer[a]

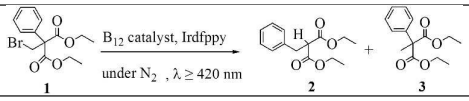

Entry	Solvent	Conversion (%)	Yield (%)		2/3	TON1	TON2
			2	3			
1	EtOH	100	8	85	0.09	270	211
2	CH_3CN	100	21	79	0.26	300	234
3	PhCN	95	50	23	2.17	219	171

[a]Condition: [B_{12} complex]=1.0×10^{-5} M, [Irdfppy]=1.28×10^{-5} M (1.28 equiv. mole), [TEOA]=0.25 M, [substrate]=3.0×10^{-3} M (300 equiv. mole), reaction time: 12 hours, light source: 200 W tungsten lump with L42 cut-off filter ($\lambda \geq 420$ nm) at 5 cm distance. Conversion and yield were based on the initial concentration of the substrate and calculated by GC-MS. TON1 is based on [B_{12} complex], TON2 is based on [Irdfppy].

The other iridium(III) complexes, Irppy, Irpbt and [Ir{dF(CF3)ppy}2(dtbpy)]PF6 and the most widely utilized visible light harvesting photosensitizer, [Ru(II)(bpy)$_3$]Cl_2, were used as photosensitizers. The results are summarized in Table 3. Catalytic efficiencies comparable to that of Irdfppy were obtained for Irpbt and [Ir{dF(CF_3)ppy}$_2$(dtbpy)]PF_6 (Entries 3 and 4 in Table 3). Some further dechlorinated products, 1,1,4,4-tetrakis(4-chlorophenyl)-2,3-dichloro-2-butene (TTDB), 1-chloro-2,2-bis(4-chlorophenyl)ethylene (DDMU) and ethyl 2,2-bis(4-chlorophenyl)acetate (DDA) were obtained in low yield (Entries 2, 3 and 4, in Table 3, Fig. S3).[¶] It is noted that the yield of DDD sharply decreased to 26% when Irdfppy was replaced by [Ru(II)(bpy)$_3$]Cl_2 as a photosensitizer (Entry 5 in Table 3). This was probably due to the gradual decomposition of [Ru(II)(bpy)$_3$]Cl_2 under visible light irradiation.

The photocatalytic system was applied to the B_{12} enzyme-mimic reaction, the 1,2-migration of the phenyl group of 2-bromomethyl-2-phenylmalonate (**1**). The results are summarized in Table 4. The phenyl migrated product, diethylbenzylmalonate (**2**), along with the simply reduced product, 2-methyl-2-phenylmalonate (**3**), were obtained and the distribution of **2** and **3** were dependent on the solvents. The ratio of **2**/**3** was 0.09 in EtOH, 0.26 in CH_3CN and 2.17 in PhCN. The ratio of **2** significantly increased in poor hydrogen radical donor solvents, which showed the same tendency as in our previous report.[18]

Table 5 Rate constants (k_{eT}) and driving forces ($-\Delta G_{eT}$) for oxidative or reductive quenching of the photosensitizers

	oxidative quenching by B_{12} complex		reductive quenching by TEOA	
	k_{eT} (10^8 M^{-1} s^{-1})	$-\Delta G_{eT}$ (eV)	k_{eT} (10^8 M^{-1} s^{-1})	$-\Delta G_{eT}$ (eV)
Irdfppy	26	0.56	9.4	0.54
[Ir{dF(CF_3)ppy}$_2$ (dtbpy)]PF_6	23	0.41	7.7	0.59
Irpbt	17	0.51	N.D.	0.28
Irppy	13	0.29	N.D.	–0.03

View Article Online
DOI: 10.1039/C7DT03742B

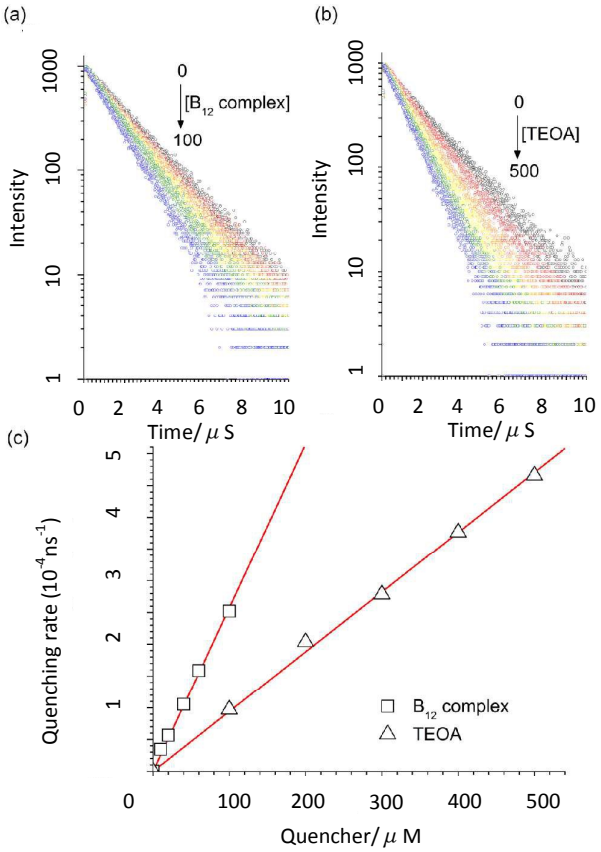

Fig. 6 (a,b) Phosphorescence decay traces of 100 μM Irdfppy (Ar-saturated CH_3CN) with increasing the concentration of B_{12} complex (a) or TEOA (b). (c) Pseudo first order fit of the quenching rate as a function of the added concentrations of B_{12} complex (squares) and TEOA (triangles).

To gain a mechanistic insight, we investigated the photoredox catalytic cycle of the iridium(III) photosensitizers. The steady-state photophysical results provided strong evidence that the B_{12} complex was reduced to a Co(I) species by the photoexcited catalyst (i.e., Fig. 2). Two electron-transfer pathways can exist in this reduction step: 1) an oxidative quenching of the photocatalyst by the B_{12} complex, and 2) a reductive quenching of the photocatalyst by TEOA, followed by transfer of the extra electron to the B_{12} complex. In the case of the oxidative quenching pathway, the one electron-oxidized photosensitizer is neutralized by electron donation by TEOA. Inspection of the electrochemical potentials in Table 1 indicated varying thermodynamic allowance of the quenching pathways. Specifically, Irdfppy, $[Ir\{dF(CF_3)ppy\}_2(dtbpy)]PF_6$ and Irpbt are predicted to follow both oxidative and reductive quenching pathways, whereas only an oxidative quenching pathway would be available for Irppy. The driving force ($-\Delta G_{eT}$) for both pathways was calculated assuming a one-electron transfer process; the oxidative quenching pathway, $-\Delta G_{eT} = e\cdot[E^*_{ox}(\text{photocatalyst}) - E_{red}(Co^{II/I})]$, and the reductive quenching pathway, $-\Delta G_{eT} = e\cdot[E_{ox}(\text{TEOA}) - E^*_{red}(\text{photocatalyst})]$. In this equation, e is the elementary charge. The calculated $-\Delta G_{eT}$ values are summarized in Table 5. It was determined that Irdfppy possesses the highest $-\Delta G_{eT}$ value for the oxidative quenching pathway, followed by Irpbt > $[Ir\{dF(CF_3)ppy\}_2(dtbpy)]PF_6$ > Irppy. In the case of the reductive quenching, $[Ir\{dF(CF_3)ppy\}_2(dtbpy)]PF_6$ is predicted to have the highest $-\Delta G_{eT}$. $-\Delta G_{eT}$ for the reductive quenching of Irdfppy is lower than that for $[Ir\{dF(CF_3)ppy\}_2(dtbpy)]PF_6$ by 0.05 eV. Judging from the negative $-\Delta G_{eT}$ (−0.03 eV), Irppy cannot undergo reductive quenching by TEOA. Note that almost identical driving forces for the oxidative and reductive quenching pathways exist in Irdfppy, and that other photocatalysts have driving forces for the oxidative quenching greater than those for the reductive quenching except for $[Ir\{dF(CF_3)ppy\}_2(dtbpy)]PF_6$.

The quenching process of the photosensitizers was directly

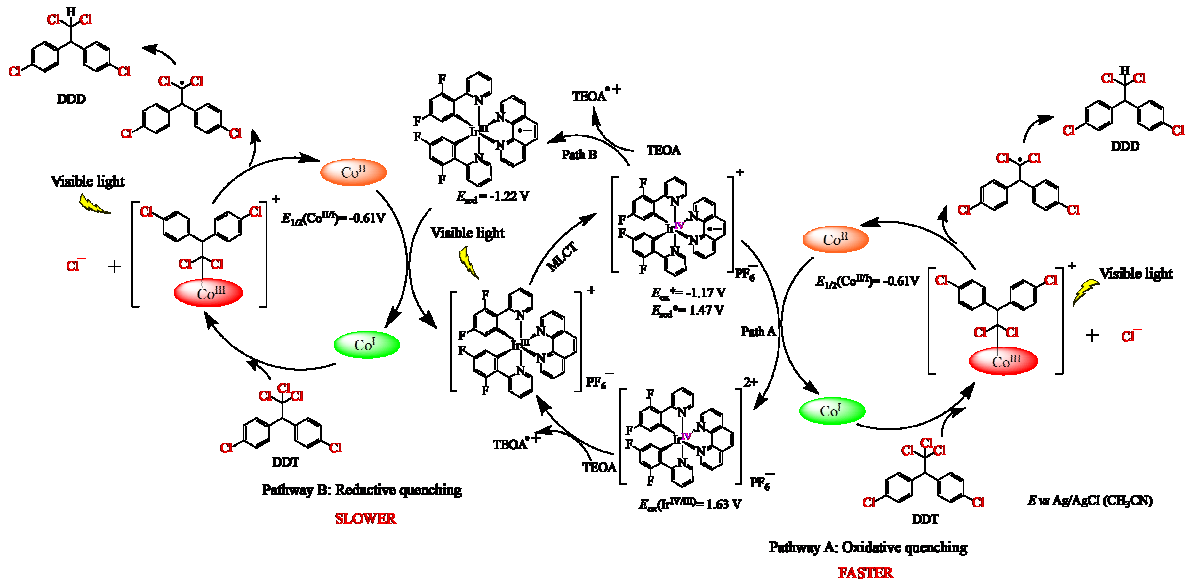

Fig. 7 Plausible reaction mechanism for the dechlorination of DDT by B_{12} complex with Irdfppy photosensitizer.

View Article Online
DOI: 10.1039/C7DT03742B

monitored by employing transient photoluminescence techniques. Photoluminescence decay traces of 100 μM Irdfppy (Ar-saturated CH_3CN) were acquired after picosecond pulsed laser photoexcitation with the increasing concentration of the B_{12} complex or TEOA (Fig. 6a,b). Pseudo first order kinetics analyses yielded the rate constant for the bimolecular one-electron transfer (k_{eT}) between the photoexcited Irdfppy and B_{12} complex (i.e., oxidative quenching pathway) or TEOA (i.e., reductive quenching pathway) (Fig. 6c). Results for the other photosensitizers are shown in Figs. S4-S6. The determined k_{eT} values are included in Table 5. It was determined that k_{eT} for the oxidative quenching ($1.3–2.6 \times 10^9$ M^{-1} s^{-1}) are greater than those for the reductive quenching ($7.7–9.4 \times 10^8$ M^{-1} s^{-1}) by two or three fold, a result consistent with the prediction based on $-\Delta G_{eT}$. This finding suggests that oxidative quenching is favored over reductive quenching. k_{eT} for the oxidative quenching roughly increases with $-\Delta G_{eT}$, indicative of the Marcus-normal region of electron transfer. Therefore, oxidative quenching will be further dominated for a photocatalyst having a high bandgap energy or a shallow oxidation potential. Among the tested photosensitizers, Irdfppy displays the highest k_{eT} values of both the oxidative and reductive quenching pathways. These kinetic behaviors may explain the best catalytic performance of Irdfppy, although other catalysis steps should be investigated for a complete understanding.

Based on these results, a plausible reaction mechanism involving Irdfppy as a photosensitizer was constructed as shown in Fig. 7. The reaction is assumed to proceed *via* two competitive pathways, the oxidative quenching pathway (pathway A) and reductive quenching pathway (pathway B). Under visible light irradiation, Irdfppy is promoted to an excited state through the metal-to-ligand charge-transfer (MLCT) transition. The excited state oxidation potential (E^*_{ox}) and the excited state reduction potential (E^*_{red}) of Irdfppy are -1.17 V *vs.* Ag/AgCl and 1.47 V *vs.* Ag/Ag/Cl, respectively (Table 1). In the case of the oxidative quenching pathway, the excited state of Irdfppy is quenched to the one-electron oxidized species by the reduction of the B_{12} complex from the Co(II) state to form the supernucleophilic Co(I) species ($E_{1/2}(Co^{II/I})$ = -0.61 V *vs.* Ag/AgCl) which is catalytically active. The corresponding alkylated complex could then be generated along with leaving of the chloride anion by the reaction of the supernucleopholic Co(I) species with the DDT substrate.[21] The cobalt-carbon bond of the alkylated complex subsequently undergoes photolysis to form the substrate radical and Co(II) species. The substrate radical reacts with hydrogen to form the dechlorinated DDD product. In the case of the reductive quenching pathway, the excited state of Irdfppy is quenched to the one-electron reduced species by the oxidation of TEOA. The redox potential of the reduced state Irdfppy is -1.22V *vs.* Ag/AgCl. Thus, the Co(II) species would be reduced to the supernucleopholic Co(I) species to catalyze the dechlorination of DDT. For these two pathways, identical driving forces exist, but k_{eT} for the oxidative quenching pathway (2.6×10^9 M^{-1} s^{-1}) is greater than that of the reductive quenching pathway (9.4×10^8 M^{-1} s^{-1}) (Table 5), thus oxidative quenching of the photosensitizer dominated over the reductive queching pathway.[#]

Conclusion

In summary, we have developed a three-component visible light induced catalytic system with the B_{12} complex as a catalyst, cyclometalated iridium(III) complex (Irdfppy, Irppy, Irpbt and $[Ir\{dF(CF_3)ppy\}_2(dtbpy)]PF_6$) as a photosensitizer and TEOA as an electron source under a N_2 atmosphere, in which an excellent catalytic efficiency was obtained. The mechanistic study suggested that the choice of an oxidative quenching pathway or a reductive quenching pathway significantly depended on the photosensitizer. Transient photoluminescence experiments revealed that the oxidative quenching of the photocatalyst dominated over the reductive quenching. This photocatalytic system was also successfully applied to the B_{12} enzyme-mimic reaction, the 1,2-migration of phenyl group of 2-bromomethyl-2-phenylmalonate. Further application of this catalytic system to other reactions is currently in progress in our laboratory.

Acknowledgements

This study was partially supported by KAKENHI Grant Numbers 23550125, JP16H01035, and JP16H04119 from the Japan Society for the Promotion of Science (JSPS) and a Grant from the Iwatani Naoji Foundation (No. 16-4313).

Notes and references

‡ Over 80% of Cl^- based on DDD was detected after the reaction by spectrophotometric determination using the mercury(II) thiocyanate method (T. M. Florence and Y. J. Farrar, *Anal. Chim. Acta*. 1971, **54**, 373).

§ Probably due to the photosensitizing catalysis of the B_{12} complex without photosensitizer, 14% of DDD was produced (Entry 3 in Table 2). See H. Shimakoshi, L. Li, M. Nishi, Y. Hisaeda, *Chem. Commun*., 2011, **47**, 10921.

§§ Decomposition of $Co(III)(DO)(DOH)Br_2$ was monitored by UV-vis (Fig. S7) and MALDI-TOF mass spectra (Fig. S8).

¶ Didechlorinated products, TTDB and DDMU could be formed by reduction of substrate radical.[2d] The selectivity of products distribution may be caused by E_{red} of photosensitizer as shown in Table 1.

In the present catalytic reaction condition with high TEOA concentration, reductive quenching pathway could be competing to oxidative quenching pathway and possible to becomes predominant pathway. The predominant pathway should be determined by the concentration of sacrificial reagent and its redox potential.

1 W. Buckel and B. T. Golding, *Chem. Soc. Rev.,* 1996, **25**, 329; (b) Vitamin B_{12} and B_{12}-Protein, ed. B. Kraütler, D. Arigoni and B. T. Golding, Wiley-VCH, Weinheim, 1998; (c) Chemistry and Biochemistry of B_{12}, ed. R. Banerjee, Wiley-Interscience, New York, 1999; (d) R. Banerjee and S. W. Ragsdale, *Annu. Rev. Biochem.,* 2003, **72**, 209; (e) T. Toraya, *Chem. Rev.*, 2003, **103**, 2095; (f) B. Kraütler and S. Ostermann, in The Porphyrin Handbook, ed. K. M. Kadish, K. M. Smith and R. Guilard, Academic Press, 2003, **11**, 229; (g) J. Bridwell-Rabb and C. L. Drennan, *Curr. Opinion Chem. Biol*., 2017, **37**, 63; (h) K. Proinsia, M. Giedyk and D. Gryko, *Chem. Soc. Rev*., 2013, **42**, 6605.

2 (a) Y. Hisaeda and H. Shimakoshi, in Handbook of Porphyrin Science, ed. K. M. Kadish, K. M. Smith and R.

View Article Online
DOI: 10.1039/C7DT03742B

Guilard, World Scientific, 2010, **10**, 313; (b) G. N. Schrauzer and E. Deutsch, *J. Am. Chem. Soc.,* 1969, **91**, 3341; (c) G. N. Schrauzer, E. Deutsch and R. J. Windgassen, *J. Am. Chem. Soc.*, 1968, **90**, 2441; (d) H. Shimakoshi, M. Tokunaga and Y. Hisaeda, *Dalton Trans.*, 2004, 878; (e) H. Shimakoshi, Y. Maeyama, T. Kaieda, T. Matsuo, E. Matsui, Y. Naruta and Y. Hisaeda, *Bull. Chem. Soc. Jpn*., 2005, **78**, 859; (f) M. Giedyk, K. Goliszewska and D. Gryko, *Chem. Soc. Rev*., 2015, **44**, 3391.

3 (a) R. L. Metcalf, New York, NY: Wiley. 1995, **14**, 524. (b) K. Kannan, S. Tanabe and R. J. Williams, *Sci. Total Environ*., 1994, **153**, 29. (c) W. R. Kelce, C. R. Stone, S. C. Laws, L. E. Gray, J. A. Kemppainen and E. M. Wilson, *Nature*, 1995, **375**, 581.

4 A. Mansouri, M. Cregut, C. Abbes, M. J. Durand, A. Landoulsi and G. Thouand. *Appl. Biochem. Biotechnol.*, 2017, **181**, 309.

5 F. Alonso, I. P. Beletskaya and M. Yus, *Chem. Rev.* 2002, **102**, 4009.

6 (a) H. Shimakoshi, M. Tokunaga, T. Baba and Y. Hisaeda, *Chem. Comm.*, 2004, **9**, 1806; (b) W. Zhang, H. Shimakoshi, N. Houfuku, X. M. Song and Y. Hisaeda, *Dalton Trans.*, 2014, 43, 13972; (c) Y. Sun, W. Zhang, J. Tong, S. Wu, D. Liu, H. Shimakoshi, Y. Hisaeda and X. M. Song, *RSC Adv*., 2017, **7**, 19197.

7 U. S. Akhtar, E. L. Tae, Y. S. Chun, I. C. Hwang and K. B. Yoon, *ACS Catal.*, 2016, **6**, 68361.

8 P. Zhang, M. Wang, Y, Na, X. Li, Y. Jiang and L. Sun, *Dalton Trans*., 2010, **39**, 1204.

9 (a) L. Flamigni, A. Barbieri, C. Sabatini, B. Ventura, F. Barigelletti, in: V. Balzani, S. Campagna (Eds.), Photochemistry and Photophysics of Coordination Compounds II, Springer, Berlin Heidelberg, 2007, 143; (b) Y. You and W. Nam, *Chem. Soc. Rev.* 2012, **41**, 7061; (c) A. Singh, K. Teegardin, M. Kelly, K. S. Prasad, S. Krishnan and J. D. Weaver, *J. Organomet. Chem*., 2015, **776**, 51.

10 (a) D. M. Schultz and T. P. Yoon, *Science*, 2014, **343**, 985; (b) C. K. Prier, D. A. Rankic and W. C. MacMillian, *Chem, Rev.* 2013, **113**, 5322. (c) S. M. Senaweera, A. Singh and J. D. Weaver, *J. Am. Chem. Soc.*, 2014, **136**, 3002. (d) K. Singh, S. J. Staig and J. D. Weaver, *J. Am. Chem. Soc.*, 2014, **136**, 5275. (e) A. Singh, A. Arora and J. D. Weaver, *Org. Lett*., 2013, **15**, 5390.

11 (a)A. Fihri, V. Artero, A. Pereira and M. Fontecave, *Dalton Trans.* 2008, **41**, 5567. (b) M. S. Lowry, J. I. Goldsmith, J. D. Slinker, R. Rohl, R. A. Pascal, Jr., G. G. Malliaras and S. Bernhard, *Chem. Mater.,* 2005, **17**, 5713.

12 J. I. Goldsmith, W. R. Hudson, M. S. Lowry, T. H. Anderson and S. Bernhard, *J. Am. Chem. Soc.* 2005, **127**, 7502.

13 (a) S. Sudharshan, R. Naidu, M. Mallavarapu and N. Bolan, *Biodegradation*, 2012, **23**, 851; (b) W. G. Kiflom, S. O. Wandiga and G. N. Kamau, *Pure Appl. Chem*., 2001, **73**, 1907.

14 L. Werthemann, ETH Zürich (No. 4097), Dissertation, Juris Druck and Velag, Zürich, 1968.

15 Y. Murakami, Y. Hisaeda and A. Kajihara, *Bull. Chem. Soc. Jpn*., 1983, **56**. 3642.

16 Y. Murakami, Y. Hisaeda, S. D. Fan and Y. Matsuda, *Bull. Chem. Soc. Jpn.*, 1989, **62**, 2219.

17 H. Woo, S. Cho, Y. Han, W.-S. Chae, Y. You and W. Nam, *J. Am. Chem. Soc*. 2013, **135**, 4771.

18 H. Shimakoshi, M. Abiru, S. I. Izumi and Y. Hisaeda, *Chem. Commun.*, 2009, **42**, 6427.

19 Y. Murakami and Y. Hisaeda, *Bull. Chem. Soc. Jpn.* 1985, **58**, 2652.

20 S. Lee, Y. You, K. Ohkubo, S. Fukuzumi and W. Nam, *Chem. Sci*. 2014, **5**, 1463.

21 H. Shimakoshi, Z. Luo, T. Inaba and Y. Hisaeda, *Dalton Trans*. 2016, **45**, 10173.

View Article Online
DOI: 10.1039/C7DT03742B

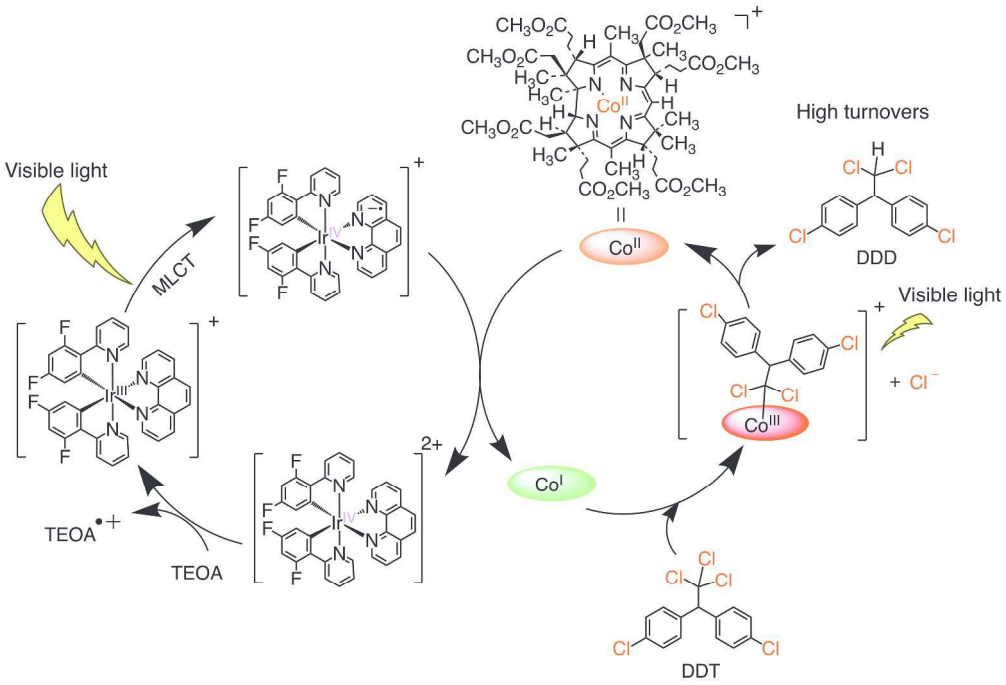

163x110mm (600 x 600 DPI)